Colloid Polym Sci (2010) 288:1393–1399
DOI 10.1007/s00396-010-2277-8

ORIGINAL CONTRIBUTION

Synthesis of microcapsules with polystyrene/ZnO hybrid shell by Pickering emulsion polymerization

Wenbao Chen · Xuyan Liu · Yangshuo Liu · Hyung-Il Kim

Received: 14 May 2010 / Accepted: 30 July 2010 / Published online: 13 August 2010

Abstract Polystyrene/zinc oxide (ZnO) hybrid microcapsules having polystyrene as inner shell and ZnO nanoparticles as outer shell were synthesized by Pickering emulsion polymerization method. ZnO nanoparticles were used to form the colloidosomes that worked as the polymerization vessels, where both styrene monomer and crosslink agent were polymerized together. Fourier transform infrared spectra and thermogravimetric thermograms showed the existence of ZnO and polystyrene in the shell of hybrid microcapsules. The hollow structure and the different morphology under various conditions were also observed by field emission scanning electron microscopy. In addition, the shell thickness of hybrid microcapsules increased as the monomer concentration increased. The photoluminescence property of PS/ZnO hybrid microcapsules could be maintained without any noticeable variation by comparing with the pure ZnO particles. It could be reasonably deduced that hybrid hollow microspheres with multifarious polymer as inner shell and ZnO nanoparticles as outer shell would be produced for many applications.

Keywords Microcapsule · Hybrid shell · Pickering emulsion · ZnO nanoparticles

W. Chen · Y. Liu · H.-I. Kim (✉)
Department of Industrial Chemistry,
Chungnam National University,
220 Gung-Dong, Yuseong-Gu,
Daejeon 305-764, South Korea
e-mail: hikim@cnu.ac.kr

X. Liu
Department of Chemical Engineering,
Chungnam National University,
220 Gung-Dong, Yuseong-Gu,
Daejeon 305-764, South Korea

Introduction

In recent years, the synthesis of hollow microspheres has attracted a great deal of attention [1–5]. The special structures of hollow microspheres made them ideal candidates for such applications as catalyst, controlled drug delivery, paints, and electronics materials [6–9]. A general approach to prepare the hollow structure is based on the layer-by-layer deposition that allows template particles to be coated by various polymeric, inorganic, and metallic materials. Other physical and chemical methods, such as colloidal crystal templating [10] and surface-initiated atom transfer radical polymerization [11], have also been developed for preparing functional hollow particles with various different materials. Based on these technologies, the design and fabrication of inorganic/polymer hybrid microspheres have attracted considerable attention recently. These hybrid particles not only exhibit special properties of inorganic components but also lead to materials with improved comprehensive properties. Strohm et al. [12] prepared polyamide hollow spheres coated with TiO_2 by liquid-phase deposition. Caruso et al. [13] had obtained inorganic hybrid hollow spheres through the colloid templated electrostatic layer-by-layer self-assembly followed by removal of the templated core. Similarly, Zhang et al. [14] synthesized SiO_2/polymer hybrid hollow microspheres via double in situ miniemulsion polymerization. Armes et al. [15] prepared the silica/polymer microspheres with a well-defined core–shell morphology by using the commercially available glycerol-functionalized ultrafine silica sol reported that using commercially available glycerol-functionalized ultrafine silica sol without surfactant or nonaqueous cosolvents.

Among all the methods mentioned, Pickering emulsions [16] were of great practical interest due to their widespread

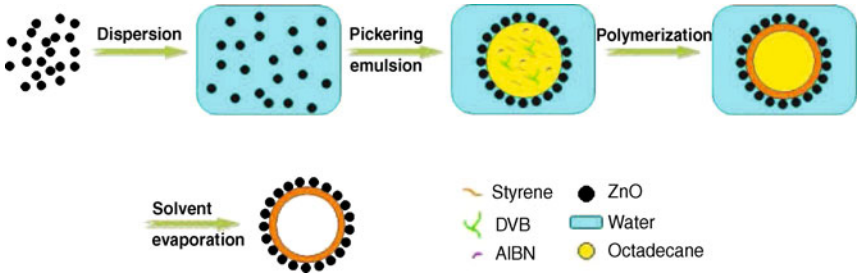

Scheme 1 Schematic illustration of the preparation of PS/ZnO hybrid microcapsules by Pickering emulsion polymerization

use in many areas including cosmetics, food, pharmaceuticals, oil recovery, and wastewater treatment. Pickering emulsion usually made robust emulsions, and it was generally difficult to break Pickering emulsions by changing the chemical or physical parameters, such as the pH, salt concentration, temperature, and composition of the oil phase. Hasell et al. [17] prepared the magnetic microparticles with poly(methyl methacrylate) core and Fe_3O_4 nanoparticle shell by Pickering suspension polymerization. He et al. [18] fabricated the novel Janus $Cu_2(OH)_2CO_3$/CuS microspheres via a Pickering emulsion route. Zhang et al. [19] made the magnetic polymer enhanced hybrid capsules from a novel Pickering emulsion polymerization. Bon et al. [20, 21] investigated solid-stabilized, or Pickering, miniemulsion polymerization using Laponite clay disks as the stabilizer for a variety of hydrophobic monomers such as styrene, lauryl methacrylate, butyl methacrylate, octyl acrylate, and 2-ethyl hexyl acrylate.

Semiconductor nanocrystals have been investigated during the past decades owing to their novel optical, electrical, and catalytic properties. The quantum confinement effect on the nanometer scale [22, 23] allowed the semiconductor nanocrystals applied in such various different fields as optoelectronics, photocatalysts, and photonic crystals [24–26]. In recent years, much attention has been paid to the zinc oxide (ZnO) nanoparticles because of its outstanding characteristics such as wide band gap of 3.37 eV at room temperature [27], photoluminescent properties [28], and fairly good conductivity [29]. Because of its unique chemical and physical properties, the ZnO nanostructure has drawn much attention in many applications, such as chemical sensors, biosensors, solar cells, photocatalysts, and optoelectronics. In this study, we prepared the polystyrene (PS)/ZnO hybrid microcapsules by a facile approach using ZnO nanoparticles as stabilizer in *o*/*w* Pickering emulsion. The unique multifarious hollow structures could be obtained by choosing the monomer and solvent as the oil phase and controlling the solubility of PS in the oil phase. Variations in morphology and property of PS/ZnO hybrid microcapsules were investigated in terms of the polymerization conditions.

Experimental

Materials

ZnO nanoparticles with mean diameter of 50 nm were obtained from Aldrich and used as stabilizer. Styrene monomer was purified by vacuum distillation. 1, 2-Divinylbenzene (DVB) as cross-linking agent, 2, 2′-azobisisbutyronitrile (AIBN) as initiator, and n-octadecane as solvent were purchased from Aldrich. These were all of analytical grade and used without any further purification.

Synthesis of PS/ZnO hybrid microcapsules

The synthetic procedures of PS/ZnO hybrid microcapsules are presented in Scheme 1. ZnO nanoparticles (0.5 g) were

Table 1 Processing parameters of Pickering emulsions for polymerization

Sample	Water phase (ml)	Oil phase				ZnO (g)
		Styrene (g)	DVB (g)	AIBN (g)	n-Octadecane (g)	
Run 1	50	0.5	0.15	0.05	1.5	0.5
Run 2	50	0.5	0.15	0.05	2.0	0.5
Run 3	50	0.5	0.15	0.05	2.5	0.5
Run 4	50	0.75	0.15	0.05	1.5	0.5
Run 5	50	1.0	0.15	0.05	1.5	0.5
Run 6	50	0.5	0.15	0.05	1.5	1.0
Run 7	50	0.5	0.10	0.05	1.5	0.5

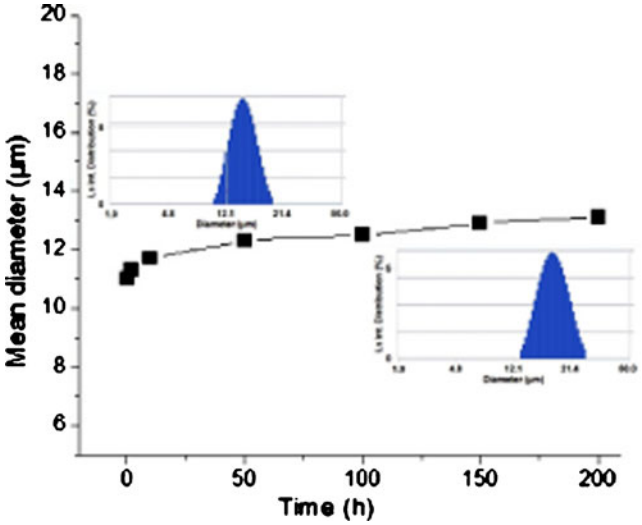

Fig. 1 Variations in the size of PS/ZnO hybrid microcapsules (run 1) depending on the time period (*insets*: size distribution of run 1 as-prepared and kept for 200 h, respectively)

dispersed in 50 ml deionized water and ultrasonicated with Branson ultrasonic cleaner (Model 2210R-DTH) at a frequency of 40 kHz for 20 min. The oil phase solutions consisting of AIBN, styrene, DVB, and n-octadecane, at the compositions shown in Table 1, were mixed with the ZnO dispersion. Pickering emulsion was prepared by vigorous stirring for 5 min at 20,000 rpm with Ika Werka Ultra Turrax T25 Basic agitator. The resultant emulsion was transferred into 100 ml round-bottomed flask. Nitrogen gas was bubbled through the emulsion for 30 min followed by heating to 55°C for the polymerization. PS/ZnO hybrid microcapsules were dried by either conventional drying at ambient temperature or freeze-drying.

Characterization

Fourier transform infrared (FTIR) spectra were recorded on a Bio-Rad FTS 175C spectrometer using KBr pellets. Ther-

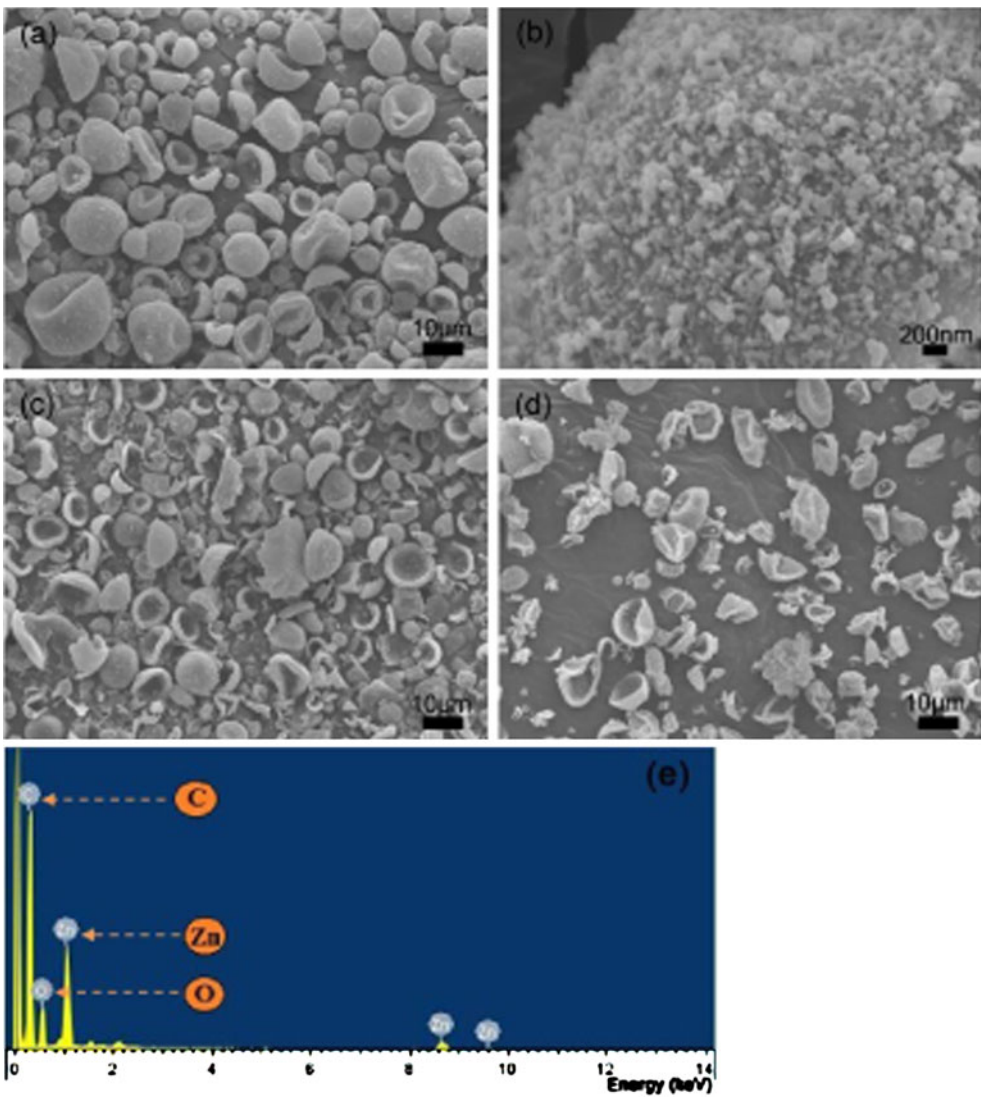

Fig. 2 SEM images of PS/ZnO hybrid microcapsules prepared from various different compositions: **a** run 1, **b** magnification of run 1, **c** run 2, **d** run 3, and **e** EDX spectrum of PS/ZnO hybrid microcapsules

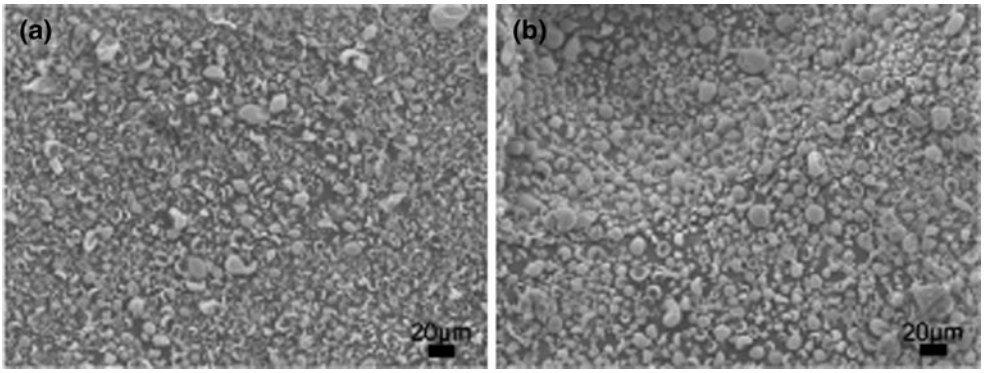

Fig. 3 SEM images of PS/ZnO hybrid microcapsules (run 5) prepared by **a** conventional drying at ambient temperature and **b** freeze-drying

mogravimetric analysis (TGA) thermograms were obtained with a TA Instrument 2050 thermogravimetric analyzer at a heating rate of 10°C/min from 25°C to 600°C under a nitrogen atmosphere. Field emission scanning electron microscopy was performed using a JEOL JSM-7000F instrument. Transmission electron microscopy (TEM) was performed using a JEM 2100F instrument. The TEM samples were prepared by dropping the dilute suspension of PS/ZnO colloid on a copper grid covered with a perforated carbon film. The room-temperature photoluminescence (PL) measurement was carried out on a Cary Eclipse fluorescence spectrophotometer and a xenon flash lamp with an excitation wavelength of 340 nm at room temperature. Energy-dispersive X-ray (EDX) microanalysis of the samples was performed during SEM measurements.

Results and discussion

Stabilization of *o*/*w* emulsions prepared with ZnO as surfactant

In order to investigate the stability of the *o*/*w* emulsions prepared with ZnO as surfactant over an extended period of time, an emulsion sample (run 1 in Table 1) was kept on the laboratory bench at room temperature for 200 h after preparation. The size and size distribution of droplets were analyzed at several different time intervals by dynamic light scattering. As shown in Fig. 1, relatively constant number averaged droplet diameter was maintained at around 12 μm during the time period of 200 h, indicating there were no severe coalescence and destabilization processes. In addition, the insets in Fig. 1 also showed that the size distribution of *o*/*w* emulsion remained relatively constant after 200 h. Hence, ZnO worked as the useful emulsifier to prepare a stable *o*/*w* emulsion, which was beneficial to the following microcapsule fabrication.

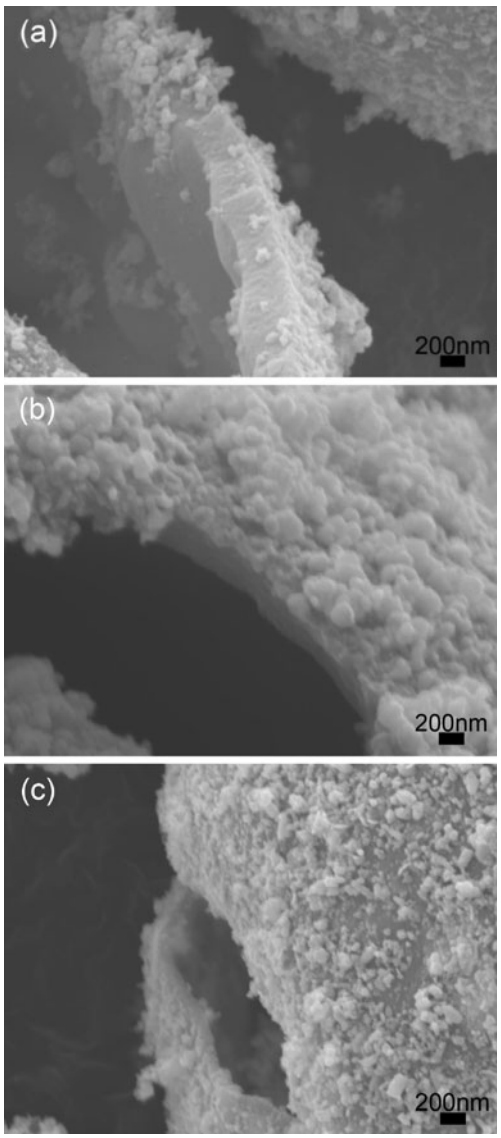

Fig. 4 SEM images of the shell of PS/ZnO hybrid microcapsules prepared with different monomer concentration: **a** run 5, **b** run 4, and **c** run 1

Morphology of PS/ZnO hybrid microcapsules

PS/ZnO hybrid microcapsules were successfully synthesized via *o*/*w* Pickering emulsion polymerization. ZnO nanoparticles as stabilizer were dispersed initially in the water phase. The *o*/*w* Pickering emulsion was formed by adding the oil phase consisting of styrene, DVB, AIBN, and n-octadecane in the aqueous ZnO dispersion. The polymerization was carried out inside the oil phase droplets. Because n-octadecane was the nonsolvent for PS, the styrene–DVB copolymer phase was separated from the reaction medium resulting in the deposition on the interface of ZnO colloidosomes to form the multifarious hollow structure. After the evaporation of solvent inside, PS/ZnO hybrid microcapsules were obtained. PS/ZnO hybrid microcapsules were shown in Fig. 2, although some of them were shrunken owing to the exhalation of solvent during the drying process. The diameters of microcapsule were in the range from 5 to 30 μm. The shell of microcapsules with ZnO nanoparticles ranging from 40 to 60 nm on the surface was clearly observed in Fig. 2b. The successful formation of PS/ZnO hybrid microcapsules was very dependent on the composition of reaction ingredients. With all the same conditions but the solvent, the solvent content was varied from 1.5 to 2.5 g. The various different morphologies of PS/ZnO hybrid microcapsules are shown in Fig. 2. As the solvent content increased in the oil phase, most of the PS/ZnO hybrid microcapsules were broken because the thinner PS walls were formed inside the ZnO colloidosomes from the diluted styrene concentration. EDX analysis was used to determine the local chemical composition of our samples.

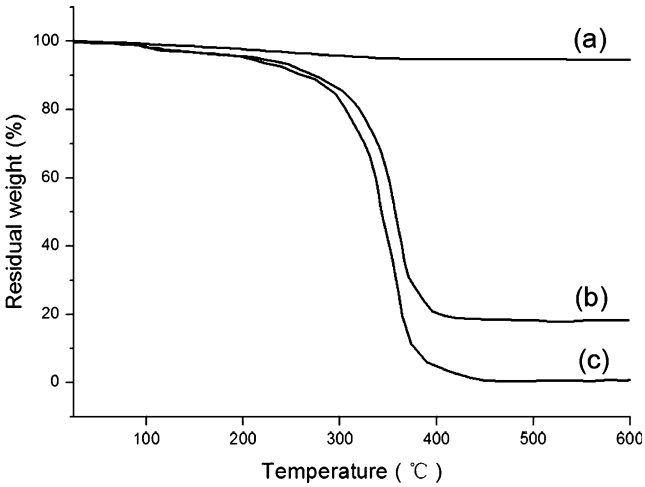

Fig. 6 TGA thermograms of **a** pristine ZnO nanoparticles, **b** ZnO/PS hybrid microcapsules (run 5), and **c** PS

EDX analysis was also carried out to determine the chemical species on the shell of PS/ZnO hybrid microcapsules. Fig. 2e shows the EDX spectrum, which exhibits the presence of Zn, O, and C elements on PS/ZnO hybrid microcapsules.

The drying method also played an important role in maintaining the microcapsule structure as shown in Fig. 3. PS/ZnO hybrid microcapsules were damaged severely by conventional drying at ambient temperature due to the pressure difference across the shell. On the other hand, the freeze-drying was effective to alleviate the stress on the shell of microcapsules during the drying process and to give most of microcapsules intact.

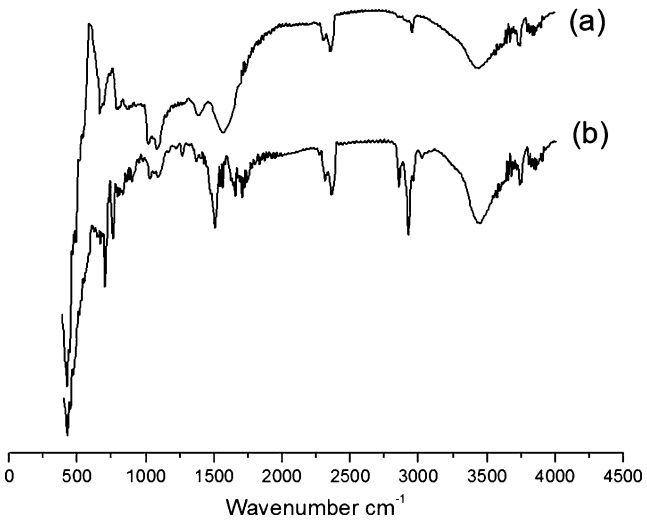

Fig. 5 FTIR spectra of **a** pristine ZnO nanoparticles and **b** PS/ZnO hybrid microcapsules (run 5)

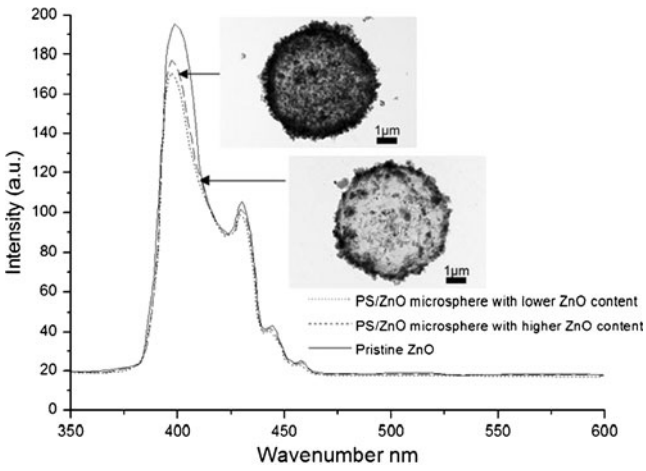

Fig. 7 PL spectra of pristine ZnO nanoparticles and PS/ZnO hybrid microcapsules. (higher ZnO content: run 6, lower ZnO content: run 1)

Effect of monomer concentration on the shell thickness of PS/ZnO hybrid microcapsules

Several different styrene monomer contents were used for the preparation of PS/ZnO hybrid microcapsules in order to study the effect of monomer concentration on the shell thickness. The monomer concentration played an important role in determining the shell thickness as shown in Fig. 4. As the monomer content decreased from 1.0 to 0.5 g in the oil phase, the shell thickness decreased from 500 to 200 nm with keeping the shape of hybrid microcapsules unaltered. Therefore, the shell thickness could be controlled easily by changing the monomer concentration in the oil phase.

Characterization of PS/ZnO hybrid microcapsules

FTIR spectra of ZnO nanoparticles and PS/ZnO hybrid microcapsules were shown in Fig. 5. For the pristine ZnO nanoparticles, the peak at 432 cm^{-1} was the characteristic absorption of Zn–O bond. The broad absorption peak at 3,437 cm^{-1} was attributed to the characteristic absorption of hydroxyl groups, and the absorptions at 1,585 and 1,423 cm^{-1} were attributed to the vibration peaks of carboxyl groups adsorbed on the surface. For the PS/ZnO hybrid microcapsules, some new vibration absorption peaks were observed at 698, 758, 1,453, 1,497, 1,601, 2,854, 2,930, and 3,016 cm^{-1}. These peaks were the typical PS absorption bands.

The thermal properties of PS/ZnO hybrid microcapsules were characterized by the TGA as shown in Fig. 6. The pristine ZnO nanoparticles showed a weight loss of about 5.8% between 25°C and 200°C due to the removal of physically adsorbed water and the decomposition of hydroxide groups. On the other hand, PS/ZnO hybrid microcapsules showed the subsequent loss of 83.7% above 200°C due to the decomposition of PS component. Furthermore, compared with the TGA plot of pure PS in Fig. 6c, the degradation temperature of PS in PS/ZnO hybrid hollow microspheres was a little higher which was resulting from the chemical or physical interaction between ZnO nanoparticles and styrene during the polymerization process.

Photoluminescence behavior of PS/ZnO hybrid microcapsules

The PL spectra of pristine ZnO nanoparticles and PS/ZnO hybrid microcapsules with both higher and lower ZnO contents were measured with an excitation wavelength of 340 nm at room temperature as shown in Fig. 7. PL spectrum of pristine ZnO showed four emission bands. A UV strong emission peak at 387 nm, corresponding to the near band edge emission, was attributed to the recombination of free excitons [30]. Peaks centering at 431, 443, and 461 nm were caused by the transition between the vacancy of oxygen and the interstitial oxygen [31]. In addition, some very weak peaks between 480 and 550 nm were attributed to the recombination of photoexcited electrons with deeply trapped holes in the singly ionized oxygen vacancy [32–34], which were responsible for the surface defects at the interface of ZnO. The PL properties of PS/ZnO hybrid microcapsules could be maintained without any noticeable variation because ZnO properties did not vary with the formation of microcapsules. ZnO worked successfully as surfactant in the preparation of PS/ZnO microcapsules without structural variation. Compared with the PL spectrum of pristine ZnO, PS/ZnO hybrid microcapsules showed nearly no change except a red shift at UV strong emission peak, which might be due to the defects and the probable shallow energy level near valence band by the introduced PS. TEM microphotographs of PS/ZnO hybrid microcapsules with different ZnO content were shown together in Fig. 7. The more ZnO nanoparticles located on the surface of microcapsules resulted in the higher intensity of PL spectra.

Conclusions

The hybrid hollow microcapsules with PS inner shell and ZnO nanoparticles outer shell were easily prepared via a Pickering emulsion reaction. The hybrid microcapsules consisting of PS and ZnO were characterized by FTIR and TGA. The various different morphologies of PS/ZnO hybrid microcapsules were observed by controlling the oil phase composition. The shell thickness of microcapsules increased as the relative monomer concentration in the oil phase increased. Compared with the pristine ZnO nanoparticles, PS/ZnO hybrid microcapsules did not show any noticeable difference in the PL spectra and maintained the good photoluminescent property. Hence, PS/ZnO hybrid microcapsules could be applied as not only chemical sensors and optoelectronics but also drug delivery systems due to the functional inorganic nanoparticles on the surface and the multifarious hollow structures.

References

1. Liu XZ, Li HJ, Ma TM, Li KZ (2009) Preparation of phenolic hollow microspheres via in situ polymerization. Polym Int 58:465–468
2. Kawashita M, Takayama Y, Kokubo T, Takaoka GH, Araki N, Hiraoka M (2006) Enzymatic preparation of hollow yttrium oxide microspheres for in situ radiotherapy of deep-seated cancer. J Am Ceram Soc 89:1347–1351
3. Qian Z, Zhang ZC, Li HM, Liu HR, Hu ZQ (2008) Facile preparation of monodisperse hollow cross-linked chitosan microspheres. J Polym Sci A Polym Chem 46:228–237

4. Zhang LJ, Wan MX, Wei Y (2006) Hollow polyaniline microspheres with conductive and fluorescent function. Macromol Rapid Commun 27:888–893
5. Han SJ, Jang BC, Kim TA, Oh SM, Hyeon TH (2005) Simple synthesis of hollow tin dioxide microspheres and their application to lithium-ion battery anodes. Adv Funct Mater 15:1845–1850
6. McQuade DT, Pullen AE, Swager TM (2000) Conjugated polymer-based chemical sensors. Chem Rev 100:2537–2574
7. Shin JM, Anisur RM, Ko MK, Im GH, Lee JH, Lee IS (2009) Hollow manganese oxide nanoparticles as multifunctional agents for magnetic resonance imaging and drug delivery. Angew Chem 121:327–330
8. Donath E, Sukhorukov GB, Caruso F, Davis SA, Möhwald H (1998) Novel hollow polymer shells by colloid-templated assembly of polyelectrolytes. Angew Chem Int Ed 37:2201–2205
9. Dong LJ, Huang J, Li R, Zhang Y, Pan MX, Xiong CX (2009) N_2-filled hollow glass beads as novel gas carriers for microcellular polyethylene. J Appl Polym Sci 114:4030–4035
10. Li HY, Meng B, Di YW, Li XY (2005) Self-assembled colloidal crystalline arrays using hollow colloidal spheres. Synthetic Met 149:225–230
11. He XY, Yang W, Yuan L, Pei XW, Gao JZ (2009) Fabrication of hollow polyelectrolyte nanospheres via surface-initiated atom transfer radical polymerization. Mater Lett 63:1138–1140
12. Strohm H, Sgraja M, Bertling J, Lobmann P (2003) Preparation of TiO2-polymer hybrid microcapsules. J Mater Sci 38:1605–1609
13. Caruso F, Caruso RA, Mohwald H (1998) Nanoengineering of inorganic and hybrid hollow spheres by colloidal templating. Science 282:1111–1114
14. Zhang JN, Yang JJ, Wu QY, Wu MY, Liu NN, Jin ZL, Wang YF (2010) SiO2/polymer hybrid hollow microspheres via double in situ miniemulsion polymerization. Macromolecules 43:1188–1190
15. Schmid A, Tonnar J, Armes SP (2008) A new highly efficient route to polymer-silica colloidal nanocomposite particles. Adv Mater 20:3331–3336
16. Pickering SU (1907) CXCVI. –Emulsions. J Chem Soc 91:2001–2021
17. Hasell T, Yang JX, Wang WX, Li J, Brown PD, Poliakoff M, Lester E, Howdle SM (2007) Preparation of polymer-nanoparticle composite beads by a nanoparticle stabilised suspension polymerization. J Mater Chem 17:4382–4386
18. He YJ, Li KS (2007) Novel Janus $Cu_2(OH)_2CO_3$/CuS microspheres prepared via a Pickering emulsion route. J Colloid Interf Sci 306:296–299
19. Zhang K, Wu W, Guo K, Chen JF, Zhang PY (2009) Magnetic polymer enhanced hybrid capsules prepared from a novel Pickering emulsion polymerization and their application in controlled drug release. Colloids Surf A 349:110–116
20. Cauvin S, Colver PJ, Bon SAF (2005) Pickering stabilized miniemulsion polymerization: preparation of clay armored latexes. Macromolecules 38:7887–7889
21. Bon SAF, Colver PJ (2007) Pickering miniemulsion polymerization using laponite clay as a stabilizer. Langmuir 23:8316–8322
22. Brus LE (1983) A simple model for the ionization potential, electron affinity, and aqueous redox potentials of small semiconductor crystallites. J Chem Phys 79:5566–5571
23. Brus LE (1984) Electron-electron and electron-hole interactions in small semiconductor crystallites: the size dependence of the lowest excited electronic state. J Chem Phys 80:4403–4409
24. Jaiswal JK, Simon SM (2004) Potentials and pitfalls of fluorescent quantum dots for biological imaging. Trends Cell Biol 14:497–504
25. Park W, King JS, Neff CW, Liddell C, Summers CJ (2002) ZnS-based photonic crystals. Phys Stat Sol (b) 229:949–960
26. Hörner G, Johne P, Künneth R, Twardzik G, Roth H, Clark T, Kisch H (1999) Semiconductor type a photocatalysis: role of substrate adsorption and the nature of photoreactive surface sites in zinc sulfide catalyzed C±C coupling reactions. Chem Eur J 5:208–217
27. Thomas DG (1960) The exciton spectrum of zinc oxide. Phys Chem Solids 15:86–96
28. Zhang JY, Feng HB, Hao WC, Wang TM (2006) Luminescent properties of ZnO sol and film doped with Tb^{3+} ion. Mat Sci Eng A: Struct 425:346–348
29. Zhang FF, Wang XL, Ai SY, Sun ZD, Wan Q, Zhu ZQ, Xian YZ, Jin LT, Yamamoto K (2004) Immobilization of uricase on ZnO nanorods for a reagentless uric acid biosensor. Anal Chim Acta 519:155–160
30. Ko HJ, Chen YF, Yao T, Miyajima K, Yamamoto A, Goto T (2000) Biexciton emission from high-quality ZnO films grown on epitaxial GaN by plasma-assisted molecular-beam epitaxy. Appl Phys Lett 77:537–539
31. Liu JP, Huang XT, Li YY, Zhong Q, Ren L (2006) Preparation and photoluminescence of ZnO complex structures with controlled morphology. Mater Lett 60:1354–1359
32. Vanheusden K, Seager CH, Warren WL, Tallant DR, Voigt JA (1996) Correlation between photoluminescence and oxygen vacancies in ZnO phosphors. Appl Phys Lett 68:403–405
33. Yin J, Lu Q, Yu Z, Wang J, Pang H, Gao F (2010) Hierachical ZnO nanorod-assembled hollow superstructures for catalytic and photoluminescence applications. Cryst Growth Des 10:40–43
34. Chen Z, Gao L (2008) A new route toward ZnO hollow spheres by a base-erosion mechanism. Cryst Growth Des 8:460–464